Catena 210 (2022) 105920

Contents lists available at ScienceDirect

Catena

journal homepage: www.elsevier.com/locate/catena

Dirt cracking as rock fracture-wedging process in the Mediterranean climate of Victoria, British Columbia, Canada

Ronald I. Dorn [a,*], Ian J. Walker [b]

[a] School of Geographical Sciences and Urban Planning, Arizona State University, Tempe, AZ 85287-5302 USA
[b] Department of Geography, University of California, Santa Barbara, CA 93106-4060, USA

ARTICLE INFO

Keywords:
Bedrock erosion
Mechanical weathering
Physical weathering
Soils
Stress loading

ABSTRACT

Dirt cracking physically wedges open fractures in desert bedrock via the synergistic processes of carbonate precipitation and the wetting and drying of clays in fracture fill. We use back-scattered and high-resolution electron microscopy along with $^{87}Sr/^{86}Sr$ analyses to find that dirt cracking also occurs in the hypermaritime Mediterranean climate of Victoria, British Columbia, Canada. $^{87}Sr/^{86}Sr$ analyses of calcium carbonate from four different sampling locations do not reflect an ocean source, but $^{87}Sr/^{86}Sr$ ratios correspond with the known composition of the sampled rocks. Carbonates derived from decay of host-rock minerals precipitate in narrow fractures, widening them. In addition to calcium carbonate, iron carbonate, barium carbonate, and calcium phosphate also precipitate in fractures. Dissolution of silicates, in association with carbonate precipitation, aids in the further penetration of carbonates. Fines falling into fissures includes smectites that undergo wetting (expansion) and drying (contraction) that further promotes fracture widening. Lead contamination, probably from mid-20th century automobile emissions, occurs from heavy metal scavenging by iron oxides. As studies of dirt cracking are few in number, and since the carbonate precipitation process has been observed in Antarctica, monsoonal Asia, and now in a Mediterranean climate, it is possible that dirt cracking is a common rock-decay process in biogeochemical settings dry enough for carbonate precipitation in rock fissures.

1. Introduction

The ubiquitous fractures found in Earth's bedrock originate through a variety of rock-forming processes, tectonic deformation, and earth-surface processes (Dubinkski and Wohl, 2013; Ehlen, 2002; Engelder, 1987; Eyles et al., 1997; Hobbs, 1967; Molnar et al., 2007; Pacheco and Alencoao, 2006; Schultz, 2000; St Clair et al., 2015; Twidale and Bourne, 1978). These weaknesses influence geomorphic processes and forms in different process domains and at different scales (Eppes et al., 2018; Scheidegger, 2001; Scott and Wohl, 2018). Although fracture widening and lengthening occur in a variety of ways (Scott and Wohl, 2018), widening can both propagate fractures and cause rock detachment (Viles, 2013). Here, we use the suggested term 'rock decay' instead of rock 'weathering' for the reasons explained elsewhere (Hall et al., 2012).

This study does not focus on initial rock-weakening processes, although they are clearly important in fracture propagation. Instead, we focus on the stress-loading process of wedging to further open existing fractures. Five general types of rock-decay processes can physically wedge open rock fractures by exerting in-crack stress loading, including: (i) frost cracking (or frost wedging) (Vliet-Lanoe and Fox, 2018; Walder and Hallet, 1986); (ii) roots and their associated fungi (Brantley et al., 2017; Gadd, 2007; Merrill, 1906); (iii) hyphae of lichens in large cracks as evidenced by incorporation of rock fragments into thalli (Scarciglia et al., 2012); (iv) salt precipitation (Oguchi and Yu, 2021; Wang et al., 2021); and (v) dirt cracking (Ollier, 1965). While frost and root fracture-wedging processes are generally well studied, dirt-cracking research is in its infancy (Dorn, 2011; Dorn, 2018; Ollier, 1965).

Originally proposed in Australia as an insolation-related thermal process (Ollier, 1965), experimental evidence and electron microscope studies revealed that the widening of desert bedrock fractures is not driven by insolation-related thermal stresses (Dorn, 2011). Instead, dirt cracking starts with the accumulation of desert dust that is ubiquitous in arid regions (Bullard and Livingston, 2009; Goudie, 1978). Dust and carbonate leached from it infiltrates down into fractures (Chitale, 1986; Coudé-Gaussen et al., 1984; Koning and Mansell, 2017; Shtober-Zisu et al., 2018; Villa et al., 1995; Wang et al., 2020) and this depositional process sets the stage for two subsequent, synergistic dirt-cracking processes that then break apart rocks. First, calcrete precipitation can

* Corresponding author.
E-mail address: ronald.dorn@asu.edu (R.I. Dorn).

https://doi.org/10.1016/j.catena.2021.105920
Received 10 June 2021; Received in revised form 17 November 2021; Accepted 25 November 2021
Available online 2 December 2021

wedge open fractures wide enough so that desert dust can begin to accumulate. Second, wetting and drying (and associated expansion and contraction (Watanabe and Sato, 1988)) of clays widen fractures to the point where spalling can occur (Dorn, 2011; Dorn, 2018; Ollier, 1965). While we would not have selected "dirt cracking" as a term for these synergistic processes, it is descriptive of what observers see in the field when they pry open rock fractures and perhaps why Ollier (1965) coined the term.

Dirt-cracking fines found inside rock fissures are not the same as skeletal or embryonic soils of rock-surface depressions (Certini et al., 2002; Darmody et al., 2008), as these contexts are subaerial as opposed to fractures within the rock. Nor are they the fracture fills found in saprolite and other *in situ* decayed rock that derive entirely from the host rock (Frazier and Graham, 2000; Thoma et al., 1992). Dirt cracking fines typically mix dust and some rock material detached from fracture walls (Dorn, 2011).

G.K. Gilbert introduced the notion of weathering-limited landscapes, arguing that the "rate of disintegration" of rocks is the limiting factor in the erosion of bare-rock desert landforms (Gilbert, 1877). Dirt cracking results in the erosion of bedrock desert landforms at rates ranging from 0.17 to 1.12 percent of bedrock surfaces spalled every thousand years. As such, dirt cracking can completely resurface the outer meter of bedrock landforms, such as bornhardts in 165–600 ka, cliff faces composed of basalt and other resistant rocks in 139–417 ka, and slick rock in ~ 93 ka (Dorn, 2018). Thus, dirt cracking is currently the most quantitatively significant physical rock decay process heretofore measured in arid landscapes.

The processes of dirt cracking — laminar carbonate growth and/or expansion/contraction of fines — have been noted in northeastern India (Vanthangliana et al., 2020); Kärkevagge in Sweden (Thorn et al., 2001), southern Siberia (Bronnikova et al., 2017), and under glaciers (Dabski et al., 2019). Dirt cracking may also be an important process on Mars (Dixon, 2018).

We present here the first study of dirt-cracking processes in a hypermaritime Mediterranean climate (Csb per the Köppen system). We use electron microscopy to study dirt-cracking processes in Victoria, British Columbia (BC), Canada, that widens bedrock fractures and thus contributes to rock decay (Fig. 1). We also employ strontium isotopes to assess whether the source of carbonate in fractures derives from marine, local rock, or a combination of the two. Although some long-range transport of Asian dust to British Columbia does occur (McKendry et al., 2001), no research in the Victoria area recognizes dust as a potential source of carbonate in the study area. The broader implication of this initial exploration is that dirt cracking could be a more widespread fracture-wedging process than understood previously.

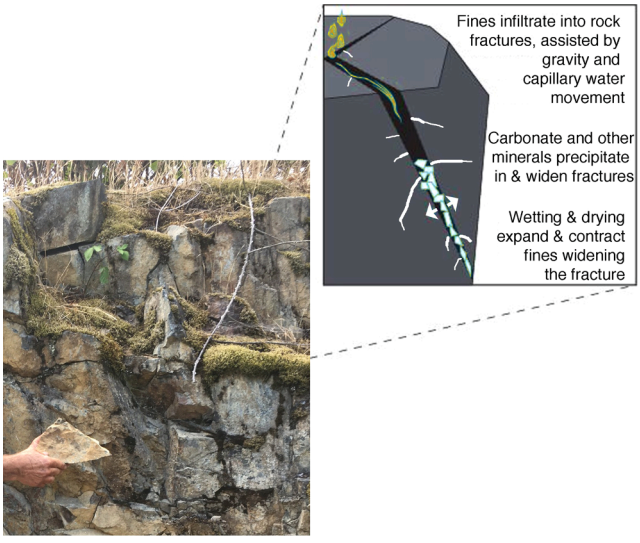

Fig. 1. Idealized diagram illustrating the processes of dirt cracking observed to occur in the hypermaritime Mediterranean climate of Victoria, BC, Canada. The photograph is from an exposure in the subsurface generated by construction. The rock itself is gneiss derived from granodiorite, but the light-colored material, being held by a hand, consists of calcium carbonate coating the walls of a rock fracture that was physically pried open during sampling. Lithobionts (e.g. mosses, lichens) take advantage of new minerals and moisture found within the expanding rock fractures.

2. Methods

2.1. Study area and sample collection sites

Victoria, BC, Canada occupies the southern tip of Vancouver Island and lies approximately 130 km south of Vancouver on mainland British Columbia; it is roughly 15–20 km from the US border with Washington state in the Strait of Juan de Fuca. According to Environment Canada's 1981–2020 climate normals for Victoria International Airport (WMO ID:71799; https://climate.weather.gc.ca/climate_normals/), the study region experiences a mean annual average temperature of 10°C (high 16.9°C in July, low 4°C in December) and a mean annual precipitation of 845.3 mm (high 148.4 mm in November, low 17.9 mm in July, 39.7 cm as snow). Per the Köppen climate classification system, Victoria's climate is temperate Mediterranean Csb due to dry (only 77.3 mm from June – August, or ~ 8.76% of annual precipitation) and warm (mean monthly temperatures < 22°C) summers.

We collected and analyzed rock samples from four locations scattered around Victoria (Fig. 2), each with varied aspects, elevation, and distance from the ocean. Hartland Landfill faces south at roughly 150 m above sea level (asl) and is roughly 6.9 km inland (west) from the ocean. Harling Point (20 m asl) and Government House (16 m asl) also face south and are within 75 m and 280 m (north) of the shoreline, respectively. The Beacon Hill site (25 m asl) faces east and is approximately 1.2 km inland (north) from the ocean. Bedrock samples were taken from exposures of both Wark and Colquitz gneiss complexes, that consists of biotite-hornblende diorite and quartz diorite (Wark) and the lighter coloured, well foliated biotite-hornblende quartz diorite to granodiorite gneiss (Colquitz) (Muller and Yorath, 1977). Collection sites were not randomly selected, but were sampled opportunistically from exposures at construction sites and bare-rock surfaces where we found visual evidence of dirt cracking. We collected *in situ* samples from both subaerial and subsurface contexts (Fig. 3). No material came from previously-opened fractures; instead, we pried fractures apart in the field to collect freshly-exposed samples.

2.2. Electron microscope methods

We employed a variety of electron microscope techniques to characterize materials within the sampled bedrock fractures. Sample preparation involved embedding a rock chip in epoxy with an orientation normal to the surface of the fracture. This positioning allows polishing of a flat surface to provide a cross-section. Backscattered electron (BSE) detectors generated images of polished surfaces where brightness reflects the average atomic number (Krinsley et al., 2005). High resolution transmission electron microscopy (HRTEM) (Krinsley et al., 1995) was used to generate nanoscale images of fracture materials. Both imaging approaches rely on energy dispersive spectroscopy (EDS) to provide elemental chemistry (Reed, 1993).

To examine potential lead concentrations, we used wavelength-dispersive spectroscopy and an electron microprobe with operating conditions of 20nA, a take-off angle of 40°, accelerating voltage of 15kv, and a 300 s counting time to increase sensitivity to a detection limit of about 0.03% weight PbO. Lead is a known constituent of contaminated rock coatings in British Columbia (Caplette and Schindler, 2018) and we were interested in determining whether lead from gasoline from the mid-20th century might have been deposited into dirt-cracking fissures

Fig. 2. Example of field collection sites with white carbonate-rich coatings on the walls of bedrock fractures in Victoria, BC at (A) Hartland landfill and (B) Harling Point. Black arrows indicate locations where fractures were mechanically pried open.

Fig. 3. Victoria, B.C., Canada, samples sites located on a Google Earth west-looking image. **A supplemental KMZ file** allows readers explore the sampling sites at much higher resolution.

at roadside locations.

2.3. Strontium isotopes

Strontium (Sr) isotopes have the potential to discriminate source materials including pedogenic and rock-decay products (Capo and Chadwick, 1999; Capo et al., 1998); the focus here rests in the origin of calcium in the carbonate in fracture fills. Sr replaces some of the calcium in calcium carbonate and, hence, is valuable to examine for understanding provenance. Because of Victoria's proximity to the Pacific Ocean, marine carbonates in sea spray could be a contributing factor. Another potential calcium source would derive from decay of the host rock. The carbonate could also derive a mixture of marine and local rock sources. While dust is a major source of calcium in desert dirt cracking (Dorn, 2011), it is not a factor in the Victoria, BC, study area.

Strontium isotope ratios cannot be used to distinguish between sources derived from rainfall or that from sea spray because both come from seawater with its $^{87}Sr/^{86}Sr$ ratio of 0.7092 (Veizer, 1989). However, $^{87}Sr/^{86}Sr$ ratios can be used to discriminate between ocean and local rock sources. Prior measurements of the major lithologic units of the Wrangellia terrane exposed on Vancouver Island range from 0.7032 to 0.7048 (Samson et al., 1990) — much lower than sea water.

Our samples, one from each site, were analyzed with a Nuclide 1290 mass spectrometer and results were normalized to the $^{87}Sr/^{86}Sr$ ratio of 0.1194 and compared to the Eimer and Amend NBS987 standard (0.7080) (Deines et al., 2003). Unlike most other analytical techniques, $^{87}Sr/^{86}Sr$ ratios do not have an instrumental error term (Capo and Chadwick, 1999; Capo et al., 1998).

3. Results

Strontium isotope $^{87}Sr/^{86}Sr$ ratios from carbonate deposits on the

fracture walls at the Beacon Hill, Harling Point, Hartland, and Government House sites (Fig. 3) are 0.70393, 0.70412, 0.70400, and 0.70399, respectively. All of these analyses rest within the range of $^{87}Sr/^{86}Sr$ ratios measured for Wrangellia terrane rocks on Vancouver Island (Samson et al., 1990). We have only one $^{87}Sr/^{86}Sr$ ratio measured from the sampled gneissic rock, from the Harling Point site — 0.70397; this ratio is only 0.00003 different from the adjacent carbonate coating. Furthermore, all of the $^{87}Sr/^{86}Sr$ ratios of the calcium carbonates are much lower than seawater. Thus, these pilot strontium isotope results suggest that the observed carbonate likely derives from host rock materials and not from seawater.

Our primary finding from electron microscope analyses is that all samples collected from the Victoria field sites showed evidence of mineral precipitates and fine materials in rock fractures. Fig. 4 presents a diagram that summarizes our basic observations, and these observations match the dirt-cracking processes observed in warm deserts (Dorn, 2011). First, calcium carbonate precipitates in sub-micron fractures. Ongoing carbonate precipitation widens the fracture enough to allow silt- and clay-sized particles into the fracture; expansive smectite clays are abundant in these fines. A positive feedback of widening and deepening fractures then allows carbonate precipitation to go deeper into a growing fracture, with then more infilling with more fines the fracture widens. The positive feedback of fracture deepening and fracture widening continues until spalling occurs. The rest of the results section elaborates on these findings.

Fig. 5 presents another typical example of what we observed, in this case from the Beacon Hill site, where calcium (with some magnesium and barium) carbonate (Fig. 5D) first precipitates in fractures (Fig. 5A-C) while incorporating mineral material from the fracture walls into the carbonate (Fig. 5B). Then, ongoing fracture widening breaks apart this coating, making room for more fines to accumulate (Fig. 5A).

Fig. 6 presents results from a sample at Beacon Hill (Fig. 1) that typifies what we see in fines that accumulate as a fracture widens. We infer a sequence of events associated with fracture widening from the BSE imagery. The fracture in Fig. 6A widens progressively as it reaches towards the subaerial rock surface, while Fig. 6B is a position deeper inside the same fracture. In both cases, white arrows highlight locations of calcium carbonate precipitation, identified by EDS analyses, that are lining the walls of the fracture. Then, after the fracture widened, fines collected inside, as illustrated by Fig. 6C. These fines, and those in other fractures, are a mixture of angular mineral matter eroded from the rock material from fracture walls and also submicron-sized particles (many of which are smectite expansive clay; see Fig. 4). Fig. 6D presents a typical EDS elemental analysis of this matrix material; Al and Si dominate, with strong peaks of Mg, Na and smaller peaks of S, Cl, K, Ca, and Fe. This elemental signature is consistent with fines containing clay minerals.

Thus, the basic nature of the dirt-cracking process involve the precipitation of carbonate and then widening of fractures associated with expansion and contraction of accumulated fines. These processes occurs in all analyzed samples with Figs. 4–6 being representative of our electron microscope results.

This research also exemplifies a methodological difficulty in analyzing dirt cracking related to sample preparation, and Fig. 7A illustrates the issue. Even careful polishing of a sample embedded in epoxy can sometimes result in evacuation of soft material from inside the fissure. The arrow in Fig. 7A identifies the location of the EDS analysis of Fig. 7**B**. This material was all that was left after very soft fracture fill eroded out during polishing, with the EDS elemental signature consistent with siderite. It would make sense that this carbonate precipitate would be much more resistant than the clay-sized matrix that eroded out during polishing.

Our findings include several new aspects about dirt cracking, not reported elsewhere in the literature. The first and most common difference compared to desert dirt cracking (e.g., Dorn, 2011) is the

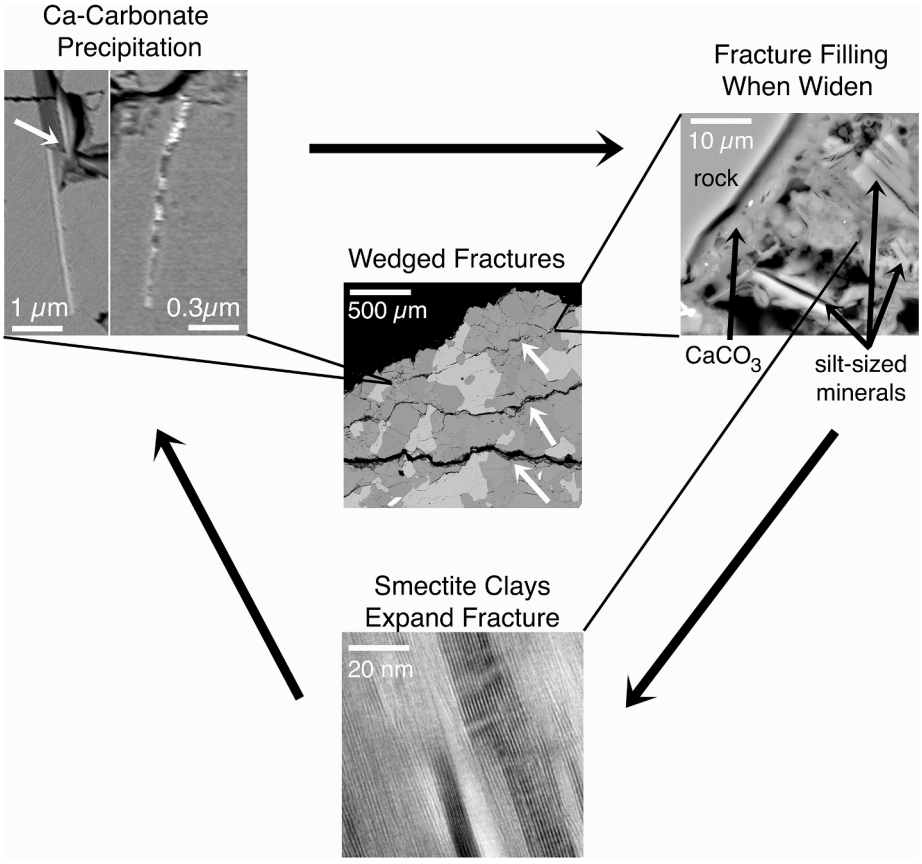

Fig. 4. Dirt cracking in Victoria, BC, consists of two processes that wedge open rock fractures. These images are from a single sample at Government House, acquired at different scales. The wedged fractures (white arrows in center BSE image) are best seen at the millimeter-scale. The calcium carbonate precipitates that fill and then begin to wedge open fractures start at the submicron scale (upper left BSE image). Once carbonate wedging opens the fracture wide enough, silt and clay-sized particles accumulate (upper right BSE image). HRTEM analyses reveal that that many of the clay-sized particles have 1.3 nm spacing indicative of smectite (Nadeau, 1985) expansive clays (lower image). The narrow black lines connecting the images indicate the location of higher resolution frames. The white arrow in the upper left image identifies a location where the laminar carbonate fractured during sample preparation, exposing a plagioclase fracture walls.

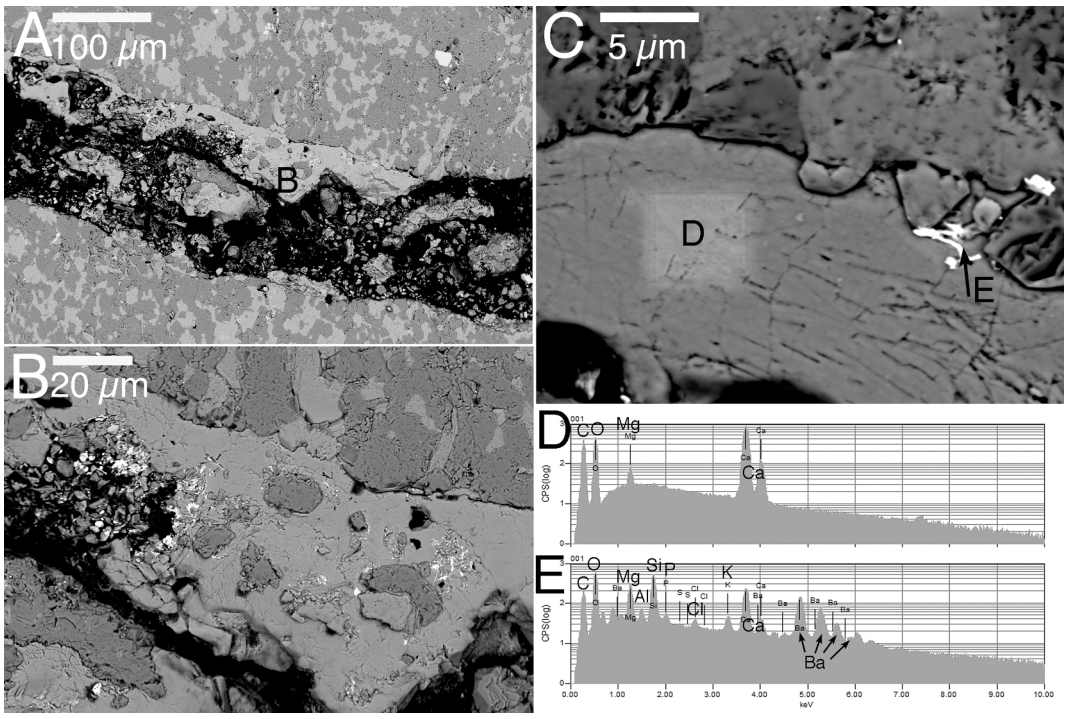

Fig. 5. Dirt cracking within the Beacon Hill site sample appears to result from carbonate wedging in open fractures. BSE images A and B show different magnifications of a fracture that first experienced carbonate precipitation and then subsequent widening. The letter B in image A is the location of the close-up Image B. Note the envelopment of fragments of rock material in the carbonate matrix. The very bright spots within the carbonate matrix is barium carbonate. The square identified by the D letter in image C is where the EDS analysis in image D was acquired; note that some minor Mg occurs along with the carbonate. The bright stringer fragment identified by the arrow and the letter E in image C identifies the location of a spot EDS analysis presented in image E. The very bright mineral has a much higher atomic number than the surrounding minerals. The narrow width of the bright stringer means that some of spectra in image E derive from the surrounding minerals; however, the 4 barium peaks along with the strong carbon and oxygen peaks suggest the bright stringer is likely barium carbonate.

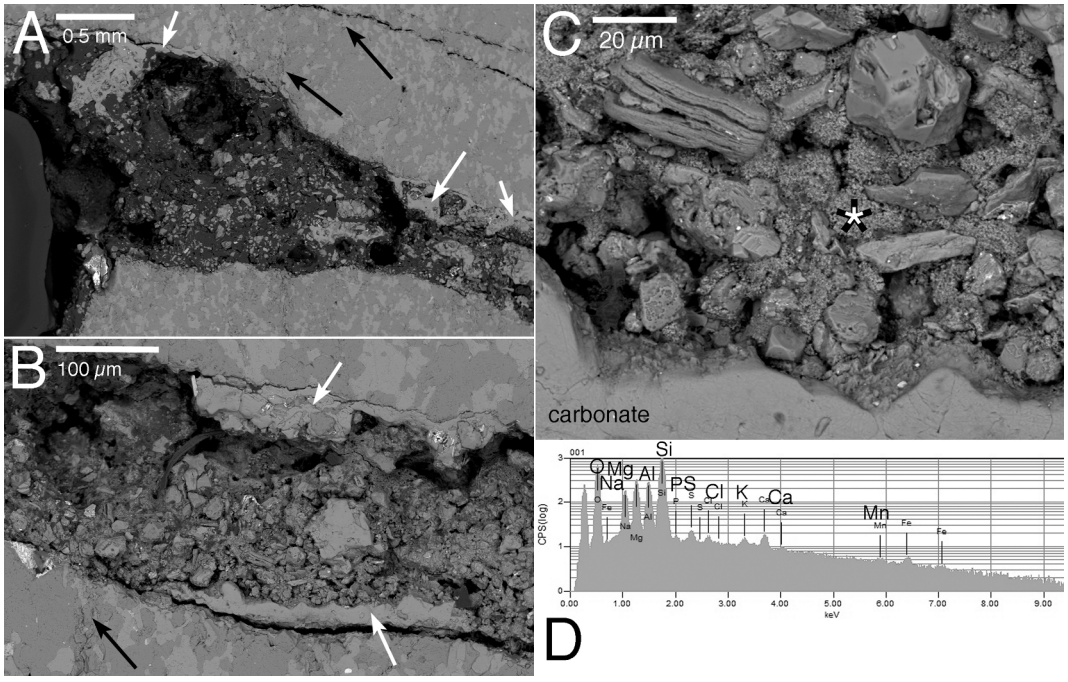

Fig. 6. BSE images at different scales reveal that the dirt cracking process at the Beacon Hill site could involve both carbonate wedging and also the accumulation of fines that subsequent undergo expansion and contraction from wetting and drying. Image A reveals that the fracture widens progressively towards the surface of the pried-open fracture. Image B shows that the widening leads to the accumulation of fines in the middle of the fracture, with carbonate attached to the fracture walls. The white arrows in Images A and B identify carbonate, while the black arrows identify smaller cracking in the rock that could be the result of ongoing widening of the dirt-cracked fracture. Image C shows a close-up view of the fines that appear to be a mix of individual silt-sized mineral particles and a matrix of clay-sized particles. The asterisk star in image C identifies the location of the EDS analysis presented in image D that is representative of this clay-sized matrix. Its composition would be consistent with a mixture of clay minerals, along with some small amounts of manganese and iron hydroxides.

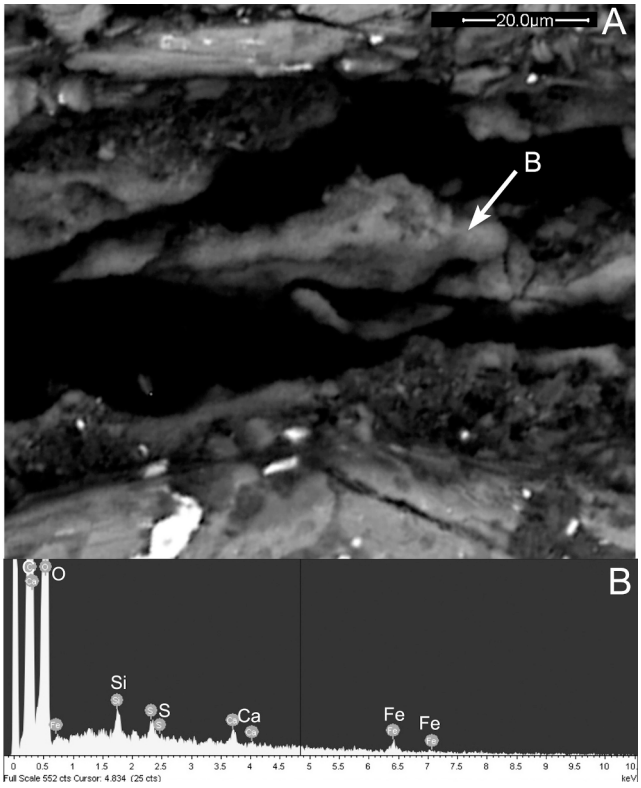

Fig. 7. Image A shows an unopened bedrock fracture from the Government House site illustrates a friable coating, possibly siderite. BSE image where the surface of the sample is adjacent to epoxy. The fracture fill at letter B and other locations still adheres to the rock material on the walls, even though much of the fill was too friable to survive the polishing process. Image B shows the EDS analysis of the coating sampled at location B in image A.

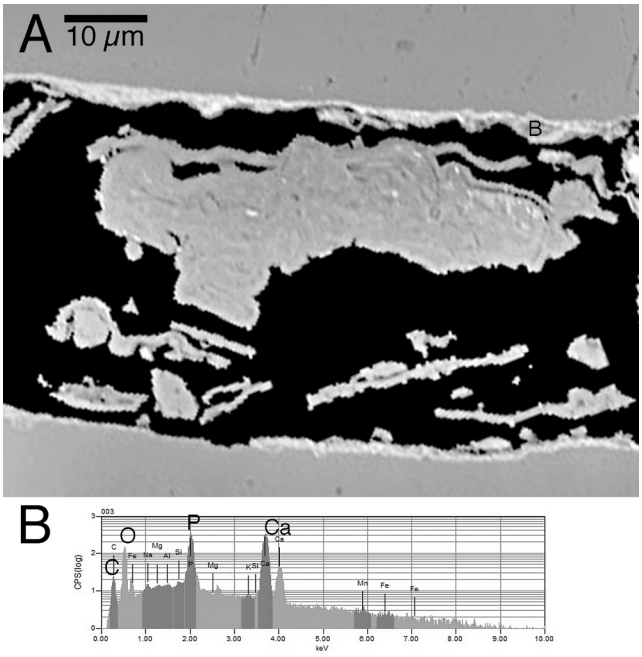

Fig. 8. The precipitates in the fractures at the Harling Point site do not appear to contain carbonate. The material attached to fracture walls and also breaking off from the fracture sides and filling in the middle appear to be a calcium phosphate mineral, perhaps apatite. Image A presents a representative BSE image of the fractures, where the location of B in image A identifies the location of the EDS analysis. The rock material itself is quartz.

occurrence of fracture precipitates other than calcium carbonate. Fig. 7B presents an EDS analysis of a fissure precipitate that is a mixture of Si, S, Ca, and Fe – along with oxygen and carbon, consistent with siderite. The white stringers in Fig. 5 appear to be a barium carbonate. A fracture precipitate at the Harling Point site (Fig. 8) is a calcium phosphate, perhaps apatite, as indicated by strong Ca and P EDS peaks. A fracture precipitate at the Hartland site in Fig. 9 contains a mixture of Si, Mg, Ca, along with Fe, Na, Al, and Ti as minor constituents (Fig. 9D). Fig. 9A also illustrates a circumstance where the fissure walls are not linear as in most joints; instead, it appears as though the precipitation of the filling simply separated feldspar from quartz.

Not every site had clear visual evidence of white carbonate on the fracture walls as seen in Fig. 1. Siderite, a ferrous carbonate, has a green–brown appearance; rubification of the fracture walls dominated the visual appearance with a hint that this reddening might be covering carbonate. Fig. 10 illustrates such a case from the Government House site. The fracture shown in Fig. 10A splits a quartz mineral. Most of the fracture fill consists of a mixture of material that appears to be clay dominated by Si, Al, Mg, and C peaks, but also with minor peaks of Ca and Fe (Fig. 10C). The bright white stringers in Fig. 10A are not carbonate, but instead appear to be a mixture of Fe and Mn (along with the clay peaks of Si, Al, and Mg) and the stronger Fe and Mn peaks give these thin deposits their brighter appearance. Thus, we speculate that rubification seen along the walls of fractures could result from these iron-rich stringers.

The Government House site exposure is a roadside location, which likely experienced frequent exposure to lead emissions from automobiles prior to December 1990, when leaded gasoline was removed from the Canadian gas market. Thus, we examined iron-rich particles imaged in Fig. 10B for lead, using the electron microprobe. Most of the non-iron material contained $<$ 0.03% PbO, the limit of detection. However, several measured iron-rich precipitates had PbO abundances well above background, illustrated by 1.22% PbO and 0.88% PbO measurements for the bright Fe-rich particles imaged in Fig. 10B. Thus, it is probable that lead pollution could have migrated into the fracture fill material and was scavenged by iron oxides. Although lead is an example of a negative anthropogenic effect, we note that it can also be useful as an indicator of decadal-scale diagenesis.

In samples with rubification along the fracture walls, calcium carbonate was not a dominant or obvious fracture precipitate. However, it still occurred in the narrowest fissures. Fig. 11 exemplifies the laminar carbonate seen in these nascent fracture precipitates, where the lower resolution BSE image in Fig. 11A reveals the carbonate to be intermittent deposits that could be precipitating and dissolving. An HRTEM image in Fig. 11B shows two nanoscale textures for the carbonate at higher resolution: a laminated texture and a more massive texture. We speculate that the carbonate is originally deposited by capillary water flow in the fractures, resulting in the more laminated or layered texture. Then, dissolution and subsequent reprecipitation around nanoscale nodes leads to the more massive carbonate appearance seen in Fig. 11B.

Nanoscale observations with HRTEM at the Hartland site reveal that fracture extension might also involve chemical processes (Eppes et al., 2018; Eppes and Keanini, 2017). Fig. 12 shows the leading edge of a fissure moving into a quartz grain. The HRTEM image reveals that extension into the quartz (Fig. 12A) is associated of nanometer-scale granules of silica (Fig. 12C). One interpretation is that the quartz is dissolving and then reprecipitating, mixing with some calcium yielding the slight Ca peak in Fig. 12C. Then, laminated calcium carbonate precipitates over the silica granules, as indicated by the strong Ca, C, and O peaks, but also with some Fe and Mg (Fig. 12B). Thus, we interpret that some expanding fractures could involve dissolution of mineral material in association with carbonate precipitation.

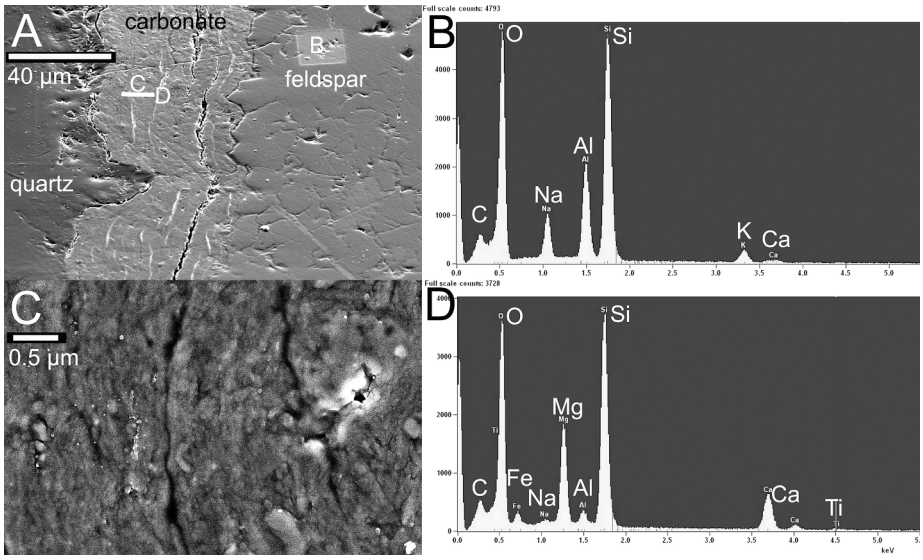

Fig. 9. An unopened fracture from the Hartland site where the walls do not appear to be linear features, but rather the physical separation of quartz from albite feldspar. The sides of the quartz and the feldspar do not match in shape, perhaps due to erosion of mineral material in a pre-existing void. Image A shows an SE image with the fracture fill separating quartz from albite feldspar. B shows EDS of the feldspar imaged at the B-box in image A. The quartz was indicated by a separate EDS analysis not shown. Image C is a close-up of the C location in image A revealing that the fill has a laminated texture. D shows an EDS of a typical composition of the fracture fill acquired at the letter D in A.

4. Discussion

Most published studies of dirt-cracking processes did not use the term "dirt cracking" coined by Ollier (1965); rather they simply refer to either carbonates that precipitate in rock fractures or the fines that accumulate in rock fractures in warm arid settings, notably in the Sahara, Simpson, Sinai Peninsula, Namib, Chihuahuan and Sonoran deserts (Amit and Gerson, 1986; Bourke and Viles, 2007; Cooke, 1970; Coudé-Gaussen et al., 1984; Koning and Mansell, 2017; Mabbutt, 1977; Moores et al., 2008; Smith, 1988; Smith, 2009; Viles, 2005; Villa et al., 1995; Williams and Robinson, 1989). Others have noted the dirt-cracking processes of carbonate precipitation or wetting/drying of fracture fill outside of warm deserts, such as Antarctica (Hall, 1989), monsoon Asia (Kiernan, 1992), and in association with wildfires (Shtober-Zisu et al., 2018). Recently, dirt cracking has also emerged as a possible geomorphic process on Mars (Chan et al., 2008; Clarke and Pain, 2004; Thomas et al., 2005). To date, however, we have not found published accounts of dirt cracking as a geomorphic mechanism of rock decay under soils or in temperate climates; both settings occur at our Victoria BC sites.

Of the five general types of wedging processes presented in the introduction, we can probably rule out salt precipitation (Oguchi and Yu, 2021; Wang et al., 2021) that does not occur away from the coastline of Victoria. However, the Harling Point site experiences abundant sea spray in winter months. Although frost cracking (Walder and Hallet, 1986) is not common in today's climate, its effect cannot be ruled out during Holocene cold events. Similarly, although we did not observe roots and their associated fungal hyphae (Gadd, 2007) or lichen thalli (Scarciglia et al., 2012) in any of our samples, we cannot rule out a paleo-lithobiontic process. While the absence of these wedging processes in our study does not rule out their possible role in the past, the clear evidence of dirt cracking processes in our samples does suggest that dirt cracking is an important wedging process in the study area.

Though the climate of Victoria, British Columbia, Canada is classified as Mediterranean, it is also hypermaritime due to the strong seasonal (fall-spring) supply of moisture from the Pacific Ocean. As such, it was surprising for us to discover dirt cracking as a rock decay process; yet it is clearly evident. These results suggest that dirt cracking might be more prevalent than previously thought and might also be found in other Mediterranean settings (Scarciglia et al., 2005; Vierra et al., 2018) as well as semi-arid (Meyer et al., 2021) climates.

Frost cracking (or frost wedging) is recognized as a process that has a positive feedback in that rates increase with fracture density (Andersen et al., 2015). Dirt cracking could have similar positive feedback effect (Fig. 4). Our results reveal that this positive feedback might also involve a synergism between mechanical and chemical processes working in tandem in that the narrowest of fractures, less than a micrometer wide, appear to have laminar carbonate that is undergoing precipitation and dissolution (Fig. 11). This could contribute to the dissolution of mineral matter at the leading edge of a fracture (Fig. 12) or, if not dissolution, at least quartz decrystallization (Pope, 1995) or even quartz hydration (Dorn et al., 2013).

Elsewhere in the semi-arid regions of western Canada, carbonates and other precipitates occur commonly and extensively in soils. For instance, semiarid grassland soils in Saskatchewan can accumulate upwards of 165 kg m^{-2} in precipitates (Landi et al., 2003) as individual particles and coatings on clasts (Wang and Anderson, 2000). Similarly, Mg-bearing pedogenic carbonates also occur in Saskatchewan soils (St Arnaud, 1979) as well as in Alberta (Miller et al., 1987). The role of these precipitates in rock decay under soils in temperate regions could represent a new area of research.

Comparison of the similarities and differences between these results with what is known about dirt cracking in warm deserts reveals the anecdotal nature of this research arena. For example, the laminar carbonate in warm deserts (Dorn, 2011) and at our study sites (Figs. 5 and 6) might be a common wedging agent. Or, the variety of other precipitates found at our Victoria sites might be just as important elsewhere, including barium carbonate (Fig. 5), a mixture of Si, Ca and Fe that could be related to silica glaze (Fig. 7), calcium phosphate (Fig. 8), and what appears to be a clay matrix (Fig. 10) with stringers of Mn-Fe rich materials.

These results could also have relevance for examining material on the walls of fractures as a record of past environmental contamination. Natural soil-formation processes in Mediterranean climates can lead to differential enhancement of heavy metals such as Pb, as well as Y, Cu, and Cr (Tangari et al., 2021). However, lead from automobile exhaust has left a legacy across the planet, contaminating areas as distant as Greenland and Antarctica (Boutron et al., 1994). In locations next to roadways (Motto et al., 1970), lead can contaminate adjacent rock surfaces through the process of heavy metal scavenging by iron oxides (Fein et al., 1999). Substantial lead enhancement occurs at one of the Victoria sites; concentrations in nanoscale iron particles exceed a percent inside dirt-cracked fractures (Fig. 10). Hence, it is possible that fractures in rocks along roadcuts could store a legacy of lead contamination left by automotive additives and contribute to an Anthropocene signature.

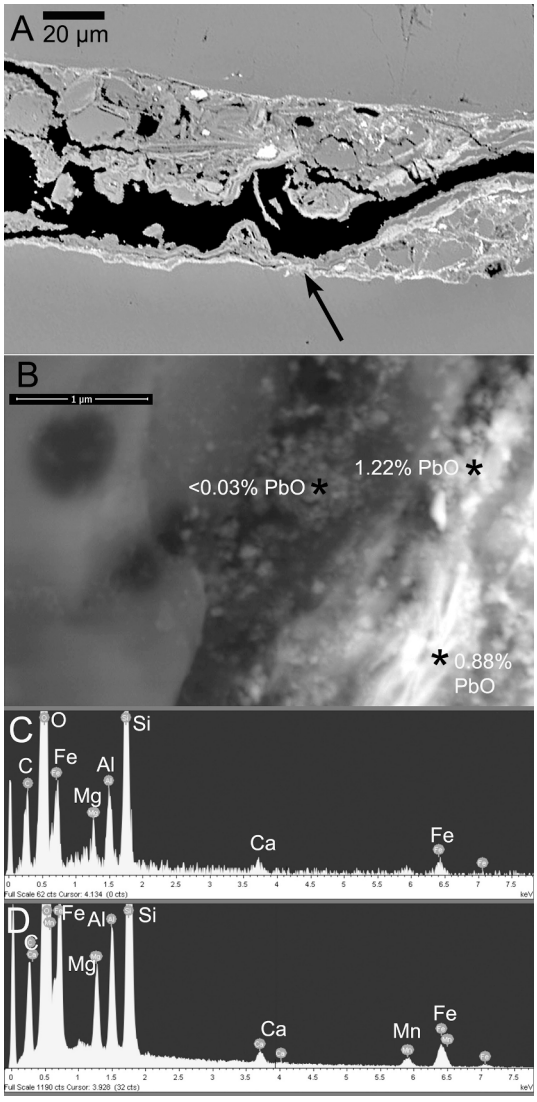

Fig. 10. Fracture fill splitting apart a quartz mineral at the Government House site. A) BSE image of a fracture fill that appears to be separating as the fracture widens. Image C presents a representative EDS spectra of the greyish fill. B) BSE close-up of the black arrow location in Image A. Image D presents a representative EDS spectra of the white stringer seen as bright fragments in this close-up. Also seen in this BSE image are the locations of focused-beam microprobe analyses for lead. While the matrix has PbO levels below background (asterisk identifies < 0.03%), several bright particles have notably high PbO concentrations of 0.88% and 1.22%. C) EDS spectra of the gray matrix of the fracture fill, indicating a composition dominated by clays (Si, Al and Mg peaks), C, and minor peaks of Ca and Fe. D) EDS spectra of image A is where the black arrow is pointing. The stronger peaks of Mn and Fe explains the brighter appearance of the stringers.

Other anthropogenic interactions are possible as well. At the Hartland Landfill site (Fig. 2), explosive blasting was likely used at the parking lot exposure in the 1990 s that we sampled (Fig. 3A). Thus, it is possible that the observed dirt cracking occurred within a few decades in an anthropogenically-generated fracture. It is also possible that the sampled fracture could have been influenced by groundwater leachate from the landfill and its management (Best et al., 2000). While our electron microscope observations at the Hartland site (Figs. 9 and 12) show no indication of either anthropogenic process, it is beyond the scope of this project to conduct the necessary joint mapping and contaminant geochemical analyses of fracture-fill material to confirm or rule out the influence of blasting or groundwater leachate.

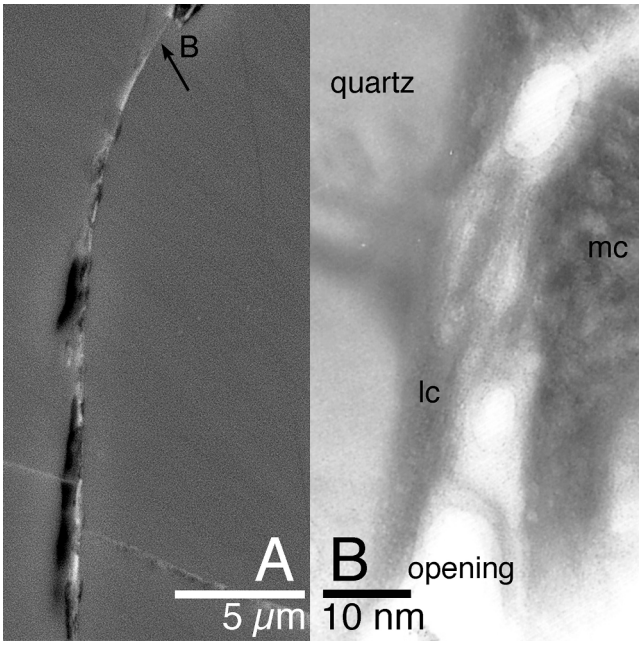

Fig. 11. The samples analyzed from the Government House site do not show any visual evidence of carbonate on the walls of fracture in hand samples or at lower resolutions using electron microscopy. However, higher resolution imagery reveals the presence of strands of carbonate precipitated in narrow fractures. A) BSE image of bright carbonate precipitates within submicron-wide fractures in quartz. The arrow and B indicate the location of image B. B) HRTEM image of a fracture in the quartz, where the fracture walls are coated with a mixture of laminar carbonate with a layered texture (lc) and also less layered, more massive carbonate texture (mc). The EDS spectra indicates a calcium carbonate composition. In this HRTEM image, the fracture opening appears the brightest, while thicker portions of the section are darker.

5. Conclusions

An examination of the first 30 powerpoint files in a Google search of college and university courses in the USA, UK and Australia that taught "physical weathering" included the following processes: expansion (pressure-release); frost wedging; root wedging; hydration/dehydration; temperature fluctuations of rock and salt; animal burrowing; salt crystal growth; and physical abrasion leading to the detachment of rock pieces. No physical rock decay ("weathering") process taught in these introductory earth science courses included dirt cracking. Perhaps it is time they should.

Most prior observations of dirt cracking — whether or not the investigator used Ollier's (1965) term — occurred in warm arid settings, notably in the Sahara, Simpson, Sinai Peninsula, Namib, Chihuahuan and Sonoran deserts (Bourke and Viles, 2007; Cooke, 1970; Coudé-Gaussen et al., 1984; Koning and Mansell, 2017; Mabbutt, 1977; Moores et al., 2008; Smith, 1988; Smith, 2009; Viles, 2005; Villa et al., 1995; Williams and Robinson, 1989). However, much more work is needed on this processes and the relevant stresses that appear to breakdown rock material outside of warm deserts.

Dirt-cracking processes (carbonate precipitation in fractures and the accumulation of expansive clays in fractures) have been observed in Antarctica (Hall, 1989), monsoon Asia (Kiernan, 1992), in association with wildfires (Shtober-Zisu et al., 2018), and as a possible process on Mars (Chan et al., 2008; Clarke and Pain, 2004; Thomas et al., 2005). Prior to this research, however, dirt cracking had not been reported in a temperate Mediterranean climate. Finding that dirt-cracking processes occur in Victoria, British Columbia, naturally leads to the possibility that dirt cracking could be much more widespread than available research suggests — at least in locations dry enough for carbonate to precipitate in rock fractures. Certainly, the time is ripe for more study of dirt

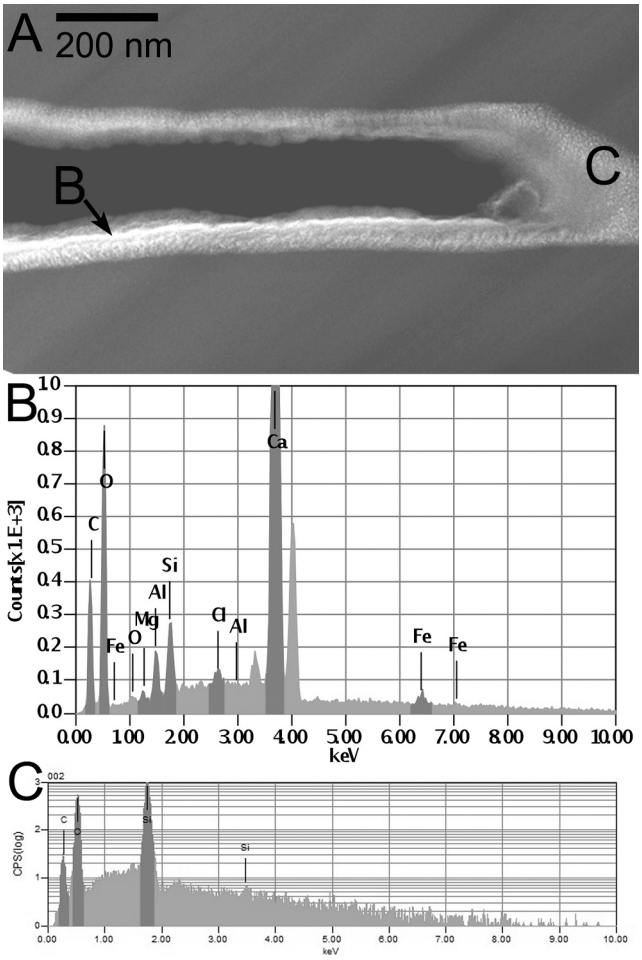

Fig. 12. Close-up of the dirt cracking process opening a fracture at the Hartland site, where the leading end of the fracture is extending into quartz. A) HRTEM image where letters B and C indicates the location of the EDS measurements. B) EDS analysis of the laminar carbonate acquired at the arrow top identified by the letter B in image A. The strong C, O and Ca peaks are consistent with a calcium carbonate composition. Minor elements include Mg, Al, Si and Cl. C) EDS analysis of the granules indicating a composition of mostly Si and O, but with some carbon.

cracking in locations that foster the development of pedocal soils (Schaetzl and Anderson, 2005).

Declaration of Competing Interest

The authors declare that they have no known competing financial interests or personal relationships that could have appeared to influence the work reported in this paper.

Appendix A. Supplementary material

Supplementary data to this article can be found online at https://doi.org/10.1016/j.catena.2021.105920. These data include Google maps of the study sites described in this article.

References

Amit, R., Gerson, R., 1986. The evolution of Holocene reg (gravelly) soils in deserts - and example from the Dead Sea region. Catena 13, 59–79.

Andersen, J.L., Egholm, D.L., Knudsen, M.F., Jansen, J.D., Nielsen, S., 2015. The periglacial engine of mountain erosion – part 1: rates of frost cracking and frost creep. Earth Surf. Dyn. 3, 447–462.

Best, M., Guy, G., Spence, G., Dosso, S., Telmer, K., 2000. Electrical anisotropy and bedrock fracturing: Is there a relationship between them? Águas Subterrâneas, 2000-09-11, https://aguassubterraneas.abas.org/asubterraneas/article/view/23926.

Bourke, M.C., Viles, H.A., 2007. A Photographic Atlas of Rock Breakdown Features in Geomorphic Environments. Planetary Science Institute, Tucson.

Boutron, C.F., Candelon, J.-P., Hong, S., 1994. Past and recent changes in the large-scale tropospheric cycles of lead and other heavy metals as documented in Antarctic and Greenland snow and ice: A review. Geochim. Cosmochim. Acta 58, 3217–3225.

Brantley, S.L., Eissenstat, D.M., Marshall, J.A., Godsey, S.E., Balogh-Brunstad, Z., Karwan, D.L., Papuga, S.A., Roering, J., Dawson, T.E., Evaristo, J., Chadwick, O., 2017. Reviews and syntheses: on the roles trees play in building and plumbing the critical zone. Biogeosciences 14, 5115–5142.

Bronnikova, M.A., Konoplianikova, Y.V., Agatova, A.R., Zazovskaya, E.P., Lebedeva, M. P., Turova, I.V., Nepop, R.K., Shorkunov, I.G., Cherkinsky, A.E., 2017. Coatings in cryoaridic soils and other records of landscape and climate changes in the Ak-Khol Lake basin (Tyva). Eurasian Soil Sci. 50, 142–157.

Bullard, J.E., Livingston, I., 2009. Dust. in: Parsons, A.J., Abrahams, A.D. (Eds.), Geomorphology of Desert Environments. Springer, New Work, pp. 629-654.

Caplette, J.N., Schindler, M., 2018. Black rock-coatings in Trail, British Columbia, Canda: Records of past emissions of lead, zinc, antimony, arsenic, tellurium, tin, selenium, silver, bismuth, and indium-bearing atmospheric contaminants. Canadian Mineralogist 56, 113–127.

Capo, R.C., Chadwick, O.A., 1999. Sources of strontium and calcium in desert soil and calcrete. Earth Planet. Sci. Lett. 170, 61–72.

Capo, R.C., Stewart, B.A., Chadwick, O.A., 1998. Strontium isotopes as tracers of ecosystem processes: theory and methods. Geoderma 82, 197–225.

Certini, G., Corti, G., Ugolini, F.C., DeSiena, C., 2002. Rock weathering promoted by embryonic soils in surface cavities. Eur. J. Soil Sci. 53, 139–146.

Chan, M.A., Yonkee, W.A., Netoff, D.I., Seiler, W.M., Ford, R.L., 2008. Polygonal cracks in bedrock on Earth and Mars: Implications for weathering. Icarus 195, 65–71.

Chitale, J.D., 1986. Study of Petrography and Internal Structures in Calcretes of West Texas and New Mexico (Microtextures, Caliche). Texas Tech University, Lubbock, p. 120 pp.. Ph.D. Dissertation. Thesis Thesis.

Clarke, J.D.A., Pain, C.F., 2004. From Utah to Mars: Regolith - landform mapping and its application. in: Cocknell, C.C. (Ed.), Martian Expedition Planning. American Astronautical Society and the British Interplanetary Society, London, pp. 131-160.

Cooke, R.U., 1970. Stone pavements in deserts. Ann. Assoc. Am. Geogr. 60, 560–577.

Coudé-Gaussen, G., Rognon, P., Federoff, N., 1984. Piegeage de poussières éoliennes dans des fissures de granitoides due Sinai oriental. Compte Rendus de l'Academie des Sciences de Paris II, 369–374.

Dabski, M., Woronko, B., Fabijańska, P., Otto, J.C., 2019. Micro-weathering of limestone surfaces in a foreland of Hallstätter Glacier (Dachstein, Austria). Geografiska Annaler: Series A Phys. Geography 101, 277–292.

Darmody, R.G., Thorn, C.E., Dixon, J.C., 2008. Differential rock weathering in the 'Valley of the Boulders', Karkevagge Swedish Lapland. Geografiska Annaler A 90A, 201–209.

Deines, P., Goldstein, S.L., Oelkers, E.H., Rudnick, R.L., Walter, L.M., 2003. Standards for publication of isotope ratio and chemical data in Chemical Geology. Chem. Geol. 202, 1–4.

Dixon, J.C., 2018. Stone pavements, lag deposits, and contemporary landscape evolution. in: Soare , R.J., Conway, S.J., Clifford, S.M. (Eds.), Dynamic Mars. Elsevier, Amsterdam, pp. 387-410.

Dorn, R.I., 2011. Revisiting dirt cracking as a physical weathering process in warm deserts. Geomorphology 135, 129–142.

Dorn, R.I., 2018. Necrogeomorphology and the life expectancy of desert bedrock landforms. Prog. Phys. Geography Earth Environ. 42, 566–587.

Dorn, R.I., Gordon, S.J., Krinsley, D., Langworthy, K., 2013. Nanoscale: Mineral weathering boundary. in: Pope, G.A. (Ed.), Treatise on Geomorphology, Vol. 4. Academic Press, San Diego, pp. 44-69.

Dubinkski, I.M., Wohl, E., 2013. Relationships between block quarrying, bed shear stress, and stream power: A physical model of block quarrying of a jointed bedrock channel. Geomophology 180–181, 55–81.

Ehlen, J., 2002. Some effects of weathering on joints in granitic rocks. Catena 91–109.

Engelder, T., 1987. Joints and shear fractures in rock. in: Atkinson, B. (Ed.), Fracture Mechanics of Rock. Academic Press, Orlando, pp. 27-69.

Eppes, M.C., Hancock, G.S., Chen, X., Arey, J., Dewers, T., Huettenmoser, J., Kiessling, S., Moser, F., Tannu, N., Weiserbs, B., Whitten, J., 2018. Rates of subcritical cracking and long-term rock erosion. Geology 46, 951–954.

Eppes, M.C., Keanini, R., 2017. Mechanical weathering and rock erosion by climate-dependent subcritical cracking. Rev. Geophys. 55, 470–508.

Eyles, N., Arnaud, E., Scheidegger, A.E., Eyles, C.H., 1997. Bedrock jointing and geomorphology in southwestern Ontario, Canada: an example of tectonic predesign. Geomorphology 19, 17–34.

Fein, J.B., Brady, P.V., Jain, J.C., Dorn, R.I., Lee, J., 1999. Bacterial effects on the mobilization of cations from a weathered Pb-contaminated andesite. Chem. Geol. 158, 189–202.

Frazier, C.S., Graham, R.C., 2000. Pedogenic transformation of fractured granitic bedrock, southern California. Soil Sci. Soc. Am. J. 64, 2057–2069.

Gadd, G.M., 2007. Geomycrology: biogeochemical transformations of rocks, minerals, metals and radionuclides by fungi, bioweathering and bioremediation. Mycol. Res. 111, 3–49.

Gilbert, G.K., 1877. Geology of the Henry Mountains. Geological and Geographical Survey, Washington D.C U.S.

Goudie, A.S., 1978. Dust storms and their geomorphological implications. J. Arid Environ. 1, 291–310.

Hall, K., 1989. Wind blown particles as weathering agents? An Antarctic example. Geomorphology 2, 405–410.
Hall, K., Thorn, C.E., Sumner, A., 2012. On the persistence of 'weathering'. Geomorphology 149–150, 1–10.
Hobbs, D.W., 1967. The formation of tension joints in sedimentary rocks: an explanation. Geol. Mag. 104, 550–556.
Kiernan, K., 1992. Geomorphological evidence for Quaternary climatic change in the low Sino-Burman ranges. Singap. J. Trop. Geogr. 12, 112–123.
Koning, D.J., Mansell, M., 2017. Rockfall susceptibility maps for New Mexico. New Mexico Bureau of Geology and Mineral Resources Open-file Report, 595, 1-41.
Krinsley, D.H., Dorn, R.I., Tovey, N.K., 1995. Nanometer-scale layering in rock varnish: implications for genesis and paleoenvironmental interpretation. J. Geol. 103, 106–113.
Krinsley, D.H., Pye, K., Boggs, S., Tovey, K.K., 2005. Backscattered electron microscopy and image analysis of sediments and sedimentary rocks. Cambridge University Press, Cambridge, U.K.
Landi, A., Mermut, A.R., Anderson, D.W., 2003. Origin and rate of pedogenic carbonate accumulation in Saskatchewan soils, Canada. Geoderma 117, 143–156.
Mabbutt, J.C., 1977. Desert landforms. Australian National University Press, Canberra.
McKendry, I.G., Hacker, J.P., Stull, R., Sakiyama, S., Mignacca, D., Reid, K., 2001. Long-range transport of Asian dust to the lower Fraser Valley, British Columbia, Canada. J. Geophys. Res. Atmospheres 106, 18361–18370.
Merrill, G.P., 1906. A treatise on rocks, rock-weathering, and soils. Macmillan, New York.
Meyer, N., Kuhwald, M., Petersen, J.F., Duttmann, R., 2021. Soil development in weathering pits of a granitic dome (Enchanted Rock) in central Texas. Catena, 199, 105084 https://www.sciencedirect.com/science/article/abs/pii/S0341816220306342.
Miller, J.J., Dudas, M.J., Longstaffe, F.J., 1987. Identification of pedogenic caronate minerals using stable carbon and oxygen isotopes, X-ray diffraction and SEM analysis. Can. J. Soil Sci. 67, 953–958.
Molnar, P., Anderson, R.S., Andersson, S.P., 2007. Tectonics, fracturing of rock, and erosion. J. Geophys. Res. Earth Surf. 112 https://doi.org/10.1029/2005JF000433.
Moores, J.E., Pelletier, J.D., Smith, P.H., 2008. Crack propagation by differential insolation on desert surface clasts. Geomorphology 102, 472–481.
Motto, H.L., Dines, R.H., Childko, D.M., Motto, C.K., 1970. Lead in soils and plants: it relationship to traffic volume and proximity to highways. Environ. Sci. Technol. 4, 231–237.
Muller, J.E., Yorath, C.J., 1977. Geology of Vancouver Island. Field Trip 7: Guidebook. . Geological Association of Canada and Mineralogical Association of Canada Joint Annual Meeting, Vancouver, G.C.
Nadeau, P.H., 1985. The physical dimensions of fundamental clay particles. Clay Miner. 20, 499–514.
Oguchi, C.T., Yu, S., 2021. A review of theoretical salt weathering studies for stone heritage. Prog. Earth Planet. Sci. 8, 1–23.
Ollier, C.D., 1965. Dirt cracking — a type of insolation weathering. Aust. J. Sci. 27, 236–237.
Pacheco, F.A.L., Alencoao, A.M.P., 2006. Role of fractures in weathering of solid rocks: narrowing the gap between laboratoryand field weathering rates. J. Hydrol. 316, 248–265.
Pope, G.A., 1995. Newly discovered submicron-scale weathering in **quartz**: Geographical implications. Professional Geographer 47 (4), 375–387.
Reed, S.J.B., 1993. Electron microprobe analysis, second ed. Cambridge University Press, Cambridge, U.K.
Samson, S.D., Patchett, J., Gehrels, G.E., Anderson, R.G., 1990. Nd and Sr Isotopic Characterization of the Wrangellia Terrane and Implications for Crustal Growth of the Canadian Cordillera. J. Geol. 98, 749–762.
Scarciglia, F., Le Pera, E., Critelli, S., 2005. Weathering and pedogenesis in the Sila Grande Massif (Calabria, South Italy): From field scale to micromorphology. Catena 61, 1–29.
Scarciglia, F., Saporito, N., La Russa, M.F., Le Pera, E., Maccione, M., Puntillo, D., Crisci, G.M., Pezzino, A., 2012. Role of lichens in weathering of granodiorite in the Sila uplands (Calabria, southern Italy). Sed. Geol. 280, 119–134.
Schaetzl, R.J., Anderson, S., 2005. Soils: Genesis and Geomorphology. Cambridge University Press, Cambridge.
Scheidegger, A.E., 2001. Surface joint systems, tectonic stresses and geomorphology: a reconciliation of conflicting observations. Geomorphology 38, 213–219.
Schultz, R.A., 2000. Growth of geologic fractures into large-strain populations: review of nomenclature, subcritical crack growth, and some implications for rock engineering. Int. J. Rock Mech. Min. Sci. 37, 403–411.
Scott, D.N., Wohl, E.E., 2018. Bedrock fracture influences on geomorphic process and form across process domains and scales. Earth Surf. Proc. Land. https://doi.org/10.1002/esp.4473, 1-19.
Shtober-Zisu, N., Brook, A., Kopel, D., Roberts, D., Ichoku, C., Wittenberg, L., 2018. Fire induced rock spalls as long-term traps for ash. Catena 162, 88–99.
Smith, B.J., 1988. Weathering of superficial limestone debris in a hot desert environment. Geomorphology 1, 355–367.
Smith, B.J., 2009. Weathering processes and forms. in: Parsons, A.J., Abrahams, A.D. (Eds.), Geomorphology of Desert Environments, 2nd edition. Springer, Amsterdam, pp. 69-100.
St Arnaud, R.J., 1979. Nature and distribution of secondary soil carbonates within landscapes in relation to soluble Mg++/Ca++ ratios. Can. J. Soil Sci. 59, 87–98.
St Clair, J., Moon, S., Holbrook, W.S., Perron, J.T., Riebe, C.S., Martel, S.J., Carr, B., Harman, C., Singha, K., deB Richter, D., 2015. Geophysical imaging reveals topographic stress control of bedrock weathering. Science, 350, 534-538.
Tangari, A.C., Le Pera, E., Ando, S., Garzanti, E., Piluso, E., Marinangeli, L., Scarciglia, F., 2021. Soil-formation in the central Mediterranean: Insight from heavy minerals. Catena 197. https://doi.org/10.1016/j.catena.2020.104998.
Thoma, S.G., Gallegos, D.P., Smith, D.M., 1992. Impact of fracture coatings on fracture/matrix flow interactions in unsaturated, porous media. Water Resour. Res. 28, 1357–1367.
Thomas, M., Clarke, J.D.A., Pain, C.F., 2005. Weathering, erosion and landscape processes on Mars identified from recent rover imagery, and possible Earth analogues. Aust. J. Earth Sci. 52, 365–378.
Thorn, C.E., Darmody, R.G., Dixon, J.C., Schlyter, P., 2001. The chemical weathering regime of Karkevagge, arctic-alpine Sweden. Geomorphology 41, 37–52.
Twidale, C.R., Bourne, J.A., 1978. Bornhardts. Zeitschrift fur Geomorphology Supplementband 31, 111–137.
Vanthangliana, V., Dinpuia, L., Walia, D., Sailo, S., Lawmkima, H., Sangi, L., Bharali, B., 2020. Polygonal Cracks in Bhuban Sandstones of Surma Basin, North East India. J. Geol. Soc. India 95, 566–570.
Veizer, J., 1989. Strontium isotopes in seawater through time. Annual Review of Earth and Planetary Sciences 17 (1), 141–167.
Vierra, E.J., Webb, H., Girty, G.H., 2018. Unravelling the development of a spheroidally weathered diorite-gabbro, Santa Margarita Ecological Reserve, Peninsular Ranges, southern California, USA. Catena 163, 297–310.
Viles, H., 2013. Synergistic weathering processes. in: Pope, G.A., Shroder, J.E.i.C. (Eds.), Treatise on Geomorphology. Volume 4. Weathering and Soils Geomorphology. Academic Press, San Diego, pp. 12-26.
Viles, H.A., 2005. Microclimate and weathering in the central Namib Desert, Namibia. Geomorphology 67, 189–209.
Villa, N., Dorn, R.I., Clark, J., 1995. Fine material in rock fractures: aeolian dust or weathering? in: Tchakerian, V. (Ed.), Desert aeolian processes. Chapman & Hall, London, pp. 219-231.
Vliet-Lanoe, B.V., Fox, C.A., 2018. Frost action. in: Stoops, G., Marelino, V., Mees, F. (Eds.), Interpretation of Micromorphological Features of Soils and Regoliths. 2nd Edition. Elsevier, Amsterdam, pp. 575-603.
Walder, J.S., Hallet, B., 1986. The physical basis of frost weathering: toward a more fundamental and unified perspective. Arct. Alp. Res. 18, 27–32.
Wang, D., Anderson, D.W., 2000. Pedogenic carbonate in Chernozemic soils and landscapes of southeastern Saskatchewan. Can. J. Soil Sci. 80, 251–261.
Wang, X., Cai, D., Zhu, B., Lou, J., Li, D., Zhang, C., Chen, S., Xu, Y., Cai, W., Su, L., Che, H., 2020. Dust-sized fractions from dustfall and physical weathering in the Gobi Desert. Aeolian Res. 43 https://doi.org/10.1016/j.aeolia.2020.100565.
Wang, Y., Viles, H., Desarnaud, J., Yang, S., Guo, Q., 2021. Laboratory simulation of salt weathering under moderate ageing conditions: Implications for the deterioration of sandstone heritage in temperate climates. Earth Surf. Proc. Land. 46, 1055–1066.
Watanabe, T., Sato, T., 1988. Expansion characteristics of montmorillonite and sapronite under various relative humidity conditions. Clay Science 7, 129–138.
Williams, R., Robinson, D., 1989. Origin and distribution of polygonal cracking of rock surfaces. Geogr. Ann. 71A, 145–159.